MONTE-CARLO MANEUVER ANALYSIS FOR THE MICROWAVE ANISOTROPY PROBE

Troy Goodson
Jet Propulsion Laboratory, California Institute of Technology

Maneuver analysis for the lunar-swingby phase of the Microwave Anisotropy Probe mission trajectories is presented. This phase spans from launch to the lunar swingby; maneuvers after the swingby are ignored. The analysis is complicated by the need to replicate the nominal trajectory in a different design tool. The results of this trajectory replication are presented, followed by the results of monte-carlo maneuver simulations. The results are subject to two important assumptions: that linearization is valid (as the software used for the monte-carlo simulation, LAMBIC, is based on a linearization of the trajectory about the nominal) and that the planned human-in-the-loop lunar targeting may be approximated by targeting to a fixed aimpoint.

INTRODUCTION

The Microwave Anisotropy Probe (MAP) project is part of NASA's Explorers program. Trajectories for MAP use a series of phasing loops to attain a lunar swingby that places the spacecraft into an orbit about the Earth-Sun L2 point. [1] Depending upon the launch date, three or five phasing loops may be used. In either case, the project's plan is to use mostly-deterministic correction maneuvers at the first and last perigees (labeled P1 and Pf, respectively) followed by a correction maneuver (PfCM) about 18 hours after Pf to ensure a lunar swingby that leads to an lissajous orbit that meets mission constraints.

The analysis described below is purely a study of maneuver targeting and the required ΔV. Trajectory analysis had been performed at Goddard Space Flight Center using Astrogator, but the Monte Carlo maneuver analysis was performed at the Jet Propulsion Laboratory (JPL) using JPL's DPTRAJ and LAMBIC software tools. DPTRAJ [2] was used to reproduce nominal trajectories and compute partial derivatives. LAMBIC was used to perform Monte-Carlo maneuver analyses. LAMBIC [3] uses linear propagation to model trajectory deviations. In other words, the effects of maneuvers are modeled with partial derivatives, as follows:

$$K_1 \Delta v_1 + K_2 \Delta v_2 + K_3 \Delta v_3 + \ldots = \Delta b,$$

where Δb is a vector of changes in the target parameters; K_i are K-matrices, matrices of partial derivatives; and Δv_i are the maneuver delta-v's. The partial derivatives, K-matrices, are supplied in a file from DPTRAJ called a K-file. The propagation options for LAMBIC are, therefore, limited only by the options in DPTRAJ for producing K-files.

LAMBIC may also optimize maneuver designs. Such designs are optimized on a per-sample basis with OD and execution errors ignored. The cost function is a sum of

ΔV magnitudes. In LAMBIC's simulation, maneuvers account for OD errors, $\Delta v_{design} = K^{-1}(\Delta b_{design} + \Delta b_{od})$, and ΔV errors are accounted for with a Gates model [4] for maneuver execution, $\Delta v_{actual} = \Delta v_{design} + \Delta v_{error}$.

The MAP project plans to adjust the aimpoint for the lunar swingby in order to achieve mission goals. This adjustment will be made by engineering judgement and is, therefore, impossible to model in LAMBIC. However, assuming this adjustment is small, a maneuver strategy that achieves the nominal aimpoint should give a fair representation of the ΔV cost for this portion of the mission.

Two cases have been studied: a three-loop case reflecting launch on May 4th, 2001 and a five-loop case reflecting launch on April 18th, 2001. The three-loop trajectory is plotted in Figure 1 and the five-loop in Figure 2. The approach used for each case is essentially identical, but the differences in the results are important.

Assumptions

The primary assumptions are high-level and as follows: linear approximation is valid and targeting to the nominal lunar swingby aimpoint is a fair representation of the project's strategy. The latter assumption has been made because engineering judgement cannot be modeled with software such as LAMBIC, although this targeting choice seems to be a reasonable compromise.
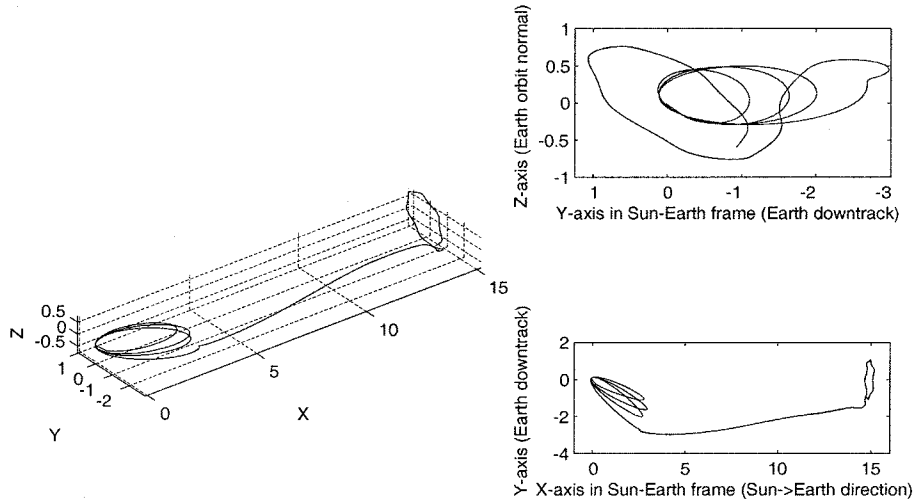
Figure 1: Trajectory for launch in May, 2001; in Sun-Earth rotating frame, scale: 1=100,000 km.

For representing injection errors, two different models were book-kept. The first was a Gates-model for injection ΔV execution errors and the second was a 6-by-6 covariance matrix (listed in the appendix). This injection ΔV execution error model consisted of a magnitude error of 11.6 m/s and a pointing error of 2 degrees, at the three-sigma level for both.

Trajectory-Correction-Maneuver (TCM) execution errors for A1, P1, Pf, and PfCM were taken to be 5% magnitude and 5 degrees pointing at the three-sigma level, per project requirements. Orbit Determination (OD) uncertainties were specified as 300 meters and 10 mm/s at the three-sigma level. These OD uncertainties were applied to the state at the data cut-off time for each maneuver design.

Analysis Approach

DPTRAJ has a capability to produce a file, called a K-file, of partial derivatives (K-matrices) that relate maneuver ΔV to encounter target conditions. This file is used by LAMBIC. Neither DPTRAJ nor LAMBIC currently has an option to modify these matrices to account for maneuver times that follow some trajectory event, viz. maneuvers that are planned to occur at perigee or apogee. As this effect is important to these cases, the DPTRAJ K-file had to be manually altered to account for it. (see appendix)

The LAMBIC software offers many options for simulating maneuvers. Unfortunately, the split-maneuver strategy that MAP plans to use is not one of the options. For the three-loop, the LAMBIC strategy chosen as the closest match to MAP's was the following: choose the P1 maneuver such that the sum of P1 ΔV and Pf ΔV magnitudes is a minimum, target the Pf maneuver to the nominal lunar swingby $\mathbf{B \cdot R}$ & $\mathbf{B \cdot T}$ ignoring the time of closest approach, and target PfCM to the same aimpoint as Pf.

For the five-loop, the LAMBIC strategy chosen as the closest match to MAP's was the following: choose the A1 maneuver such that the sum of A1, P1, and Pf ΔV magnitudes is a minimum and that the P1 altitude is greater than 510 km; choose the P1 maneuver such that the sum of P1 and Pf ΔV magnitudes is a minimum; target the Pf maneuver to the nominal lunar swingby $\mathbf{B \cdot R}$ & $\mathbf{B \cdot T}$ ignoring the time of closest approach; finally target PfCM in the same manner as Pf.

These strategies, like the MAP team's maneuver design strategy in Astrogator, have flexibility in the time of lunar closest-approach. The amount of variation in the closest-approach time is indicated by the variation in the linearized time-of-flight (LFT), quoted in the simulation results, below.

Note that although there was some initial consideration of a strategy that would allow LAMBIC to pick a lunar-swingby aimpoint such that a future Cartesian state be near the L2 point, this strategy was rejected. LAMBIC uses partial derivatives to linearly propagate the trajectory and this linear propagation does not have enough accuracy over such an arc to inspire confidence in the results. Furthermore, no attempt has been made to estimate the ΔV required to attain an L2 orbit based on the lunar delivery statistics in the Monte Carlo analysis.
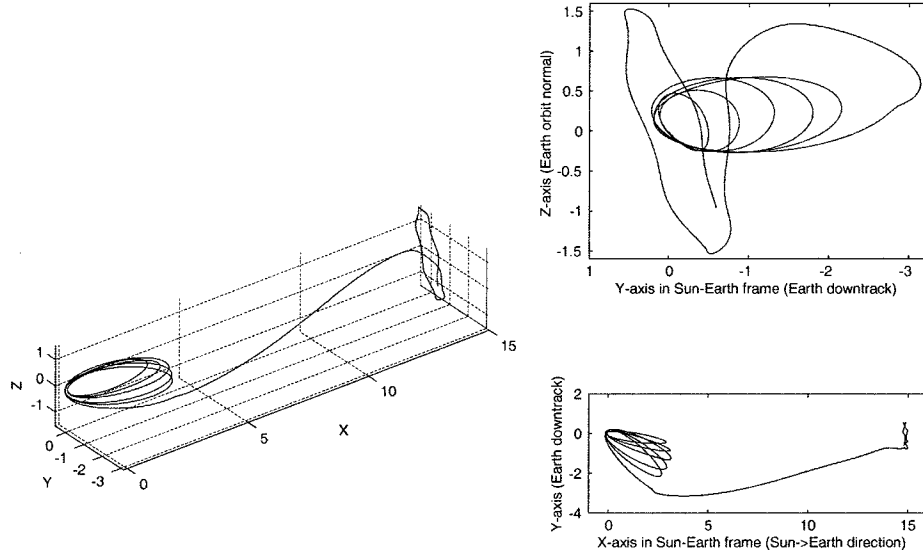
Figure 2: Trajectory for launch in April, 2001; in Sun-Earth rotating frame, scale: 1=100,000 km.

At the same time, the strategy presented here only attempts to return to the nominal lunar swingby aimpoint. The MAP navigation team plans to adjust this aimpoint to achieve mission goals. This discrepancy between the LAMBIC strategy and the MAP navigation strategy cannot be resolved because the latter is human-in-the-loop.

SIMULATION IN DPTRAJ

As the trajectories had to be reproduced in DPTRAJ in order to compute the necessary partial derivatives for LAMBIC, a comparison of results is relevant. For both launch cases, three different trajectory simulations from Astrogator were available: nominal launch, a +3-sigma magnitude error (11.6 m/s) on the ΔV from the third stage, and a −3-sigma magnitude error on the ΔV from the third stage. Aspects of these trajectories that are important in this report are listed in Table 1 and Table 2. The trajectory designs have been optimized for the +3-sigma magnitude error, which is why the total ΔV for this case is the least.

It is important to note the strategy by which the trajectories were designed using Astrogator. The P1 and Pf maneuvers were constrained to act along the local velocity directions. The desired **B•R** and **B•T** of the lunar swingby are matched by appropriately choosing the magnitudes of these maneuvers. In the five-loop case, a maneuver has been placed at A1 to satisfy a lower-bound on the perigee altitude of 510 km. These maneuvers were determined in a different manner under DPTRAJ's trajectory-search software.

The trajectory-search software in DPTRAJ is named SEPV. SEPV does not offer the exact same feature set for searching-in maneuver ΔV as Astrogator. However this is only a trajectory replication problem, not an optimization problem. For the three-loop case launching in May, reasonable agreement was found by allowing additional small

4

ΔV's: one near injection and another at A1. The Pf (P3 for the May 4th case) maneuver ΔV was copied from the Astrogator output file and input to DPTRAJ as a fixed ΔV. The near-injection ΔV was searched-in to match the Cartesian position at A1. The P1 ΔV was searched-in to match the Cartesian position at A2. A P2 ΔV was searched-in to match the B•R and B•T of the lunar swingby. For the five-loop case launching in April, the P1 maneuver ΔV was copied from the Astrogator output and input to DPTRAJ as a fixed ΔV. The A1 ΔV was searched-in to match the Cartesian position at P1. The Pf ΔV (P5 for April 18th case) was searched-in to match the Cartesian state listed in Astrogator's output, in Earth's mean equator of J2000.0 (EME2000), at the time of the lunar swingby.

Table 1. Three-Loop (May 4th launch) Trajectory Characteristics (Astrogator).
Times are UTC; B•R, B•T in EME2000.

	-3-sigma	Nominal	+3-sigma
Injection ΔV	3,088.8 m/s	3,100.4 m/s	3,112.0 m/s
A1 epoch	7-May 12:30:57	7-May 23:43:29	8-May 13:47:37
P1 epoch	10-May 12:46:44	11-May 11:10:49	12-May 15:31:01
P1 ΔV	32.6650 m/s	15.427 m/s	4.744 m/s
A2 epoch	14-May 21:43:33	15-May 14:56:24	16-May 12:45:46
P2 epoch	19-May 06:48:12	19-May 18:47:52	20-May 10:04:51
A3 epoch	23-May 16:05:08	23-May 22:41:32	24-May 07:16:36
P3 epoch	28-May 01:31:30	28-May 02:45:06	28-May 04:37:58
P3 ΔV	8.1423 m/s	12.844 m/s	19.404 m/s
Moon TCA	2-Jun 05:51:31	2-Jun 06:05:11	2-Jun 06:32:50
Moon B•R	-253.58 km	-306.97 km	-398.47 km
Moon B•T	7,324.7 km	7,526.4 km	7,738.0 km
Moon V∞	0.87352 km/s	0.86282 km/s	0.85433 km/s

The trajectories from Astrogator accounted for the gravitational attraction of the Sun, Moon, and Jupiter as point masses. For Earth's gravity, a 21-by-21 JGM-2 model [5] was used. Solar radiation pressure was modeled. Numerical integration was by the Runge-Kutta-Verner 8(9) method.

Two different simulations were run in DPTRAJ, one to produce partial derivatives for LAMBIC, and a second to match the Astrogator trajectory. The latter used a 21-by-21 JGM-2 for Earth; all gravitational influences but Earth, Moon, Sun, and Jupiter were neglected; and solar radiation pressure was modeled. The former used a 2-by-2 JGM-3 model [6] for Earth's gravity, no planet's gravity was neglected, and solar radiation pressure was not modeled.

As an additional verification, the +3-sigma launch case was reproduced in DPTRAJ using the former modeling strategy (2-by-2 JGM-3, no planets neglected, and solar pressure not modeled). In this case, the trajectory was only searched-in up to the lunar swingby.

Of course, because of implementation issues, the modeling can never be quite the same for DPTRAJ and Astrogator; but this does not mean the results of the comparison are less valuable. Selected trajectory characteristics are compared in Tables 3 through 6. These results indicate that DPTRAJ and Astrogator are simulating essentially the same trajectory.

Table 2. Five-Loop (April 18th launch) Trajectory Characteristics (Astrogator).
Times are UTC; B•R, B•T in EME2000.

	-3-sigma	Nominal	+3-sigma
Injection ΔV	3,088.9 m/s	3,100.5 m/s	3,112.1 m/s
A1 epoch	21-Apr 11:13:27	21-Apr 21:41:45	22-Apr 11:07:21
A1 ΔV	7.9701 m/s	6.9504 m/s	5.4143 m/s
P1 epoch	24-Apr 09:47:18	25-Apr 06:44:26	26-Apr 09:35:34
P1 ΔV	24.436 m/s	11.384 m/s	0.18219 m/s
A2 epoch	28-Apr 08:43:13	29-Apr 03:56:45	30-Apr 06:53:17
P2 epoch	2-May 07:38:46	3-May 01:07:57	4-May 04:08:04
A3 epoch	7-May 02:14:33	7-May 11:17:45	8-May 06:50:07
P3 epoch	12-May 12:04:54	11-May 18:48:57	12-May 09:27:54
A4 epoch	15-May 22:22:36	16-May 02:57:37	16-May 12:52:57
P4 epoch	20-May 08:45:53	20-May 11:11:29	20-May 16:23:10
A5 epoch	24-May 18:52:54	24-May 19:08:53	24-May 19:36:11
P5 epoch	29-May 05:17:28	29-May 03:23:21	28-May 23:00:52
P5 ΔV	13.692 m/s	13.795 m/s	13.410 m/s
Moon TCA	1-Jun 19:50:06	1-Jun 21:59:32	2-Jun 00:14:03
Moon B•R	-3,866.1 km	-2,272.9 km	-1,277.5 km
Moon B•T	12,786 km	12,723 km	12,775 km
Moon V_∞	0.83125 km/s	0.81414 km/s	0.82732 km/s

Table 3. Three-Loop Trajectory Comparison, Nominal Launch. Times in UTC.

	Astrogator	DPTRAJ JGM-2	DPTRAJ JGM-3 2×2
Injection ΔV	3,100.4 m/s	3100.4	3100.4 m/s
A1 epoch	7-May 23:43:29	7-May 23:43:30	7-May 23:43:25
P1 epoch	11-May 11:10:49	11-May 11:10:51	11-May 11:10:40
P1 ΔV	15.427 m/s	15.477 m/s	16.455 m/s
A2 epoch	15-May 14:56:24	15-May 14:56:29	15-May 14:56:08
P2 epoch	19-May 18:47:52	19-May 18:47:60	19-May 18:47:26
P2 ΔV	N/A	0.0 m/s	0.681 m/s
A3 epoch	23-May 22:41:32	23-May 22:41:42	23-May 22:41:03
P3 epoch	28-May 02:45:06	28-May 02:45:18	28-May 02:44:30
P3 ΔV	12.844 m/s	12.844 m/s	12.844 m/s
Moon TCA	2-Jun 06:05:11	2-Jun 06:05:13	2-Jun 06:05:05

Table 4: Three-Loop Trajectory Comparison, +3-Sigma Case. Times are UTC.

	Astrogator	DPTRAJ JGM-3 2×2
Injection ΔV	3,112.0 m/s	3,112.1 m/s
A1 epoch	8-May 13:47:37	8-May 13:47:32
P1 epoch	12-May 15:31:01	12-May 15:30:49
P1 ΔV	4.744 m/s	4.752 m/s
A2 epoch	16-May 12:45:46	16-May 12:45:27
P2 epoch	20-May 10:04:51	20-May 10:04:22
P2 ΔV	N/A	0.346 m/s
A3 epoch	24-May 07:16:36	24-May 07:16:04
P3 epoch	28-May 04:37:58	28-May 04:37:19
P3 ΔV	19.404 m/s	19.404 m/s
Moon TCA	2-Jun 06:32:50	2-Jun 06:32:38

Table 5. Five-Loop Trajectory Comparison, Nominal Launch. Times are UTC.

	Astrogator	DPTRAJ JGM-2	DPTRAJ JGM-3
A1 epoch	21-Apr 21:41:45	21-Apr 21:41:45	21-Apr 21:41:31
A1 ΔV	6.9504 m/s	6.9570 m/s	6.9582 m/s
P1 epoch	25-Apr 06:44:26	25-Apr 06:44:26	25-Apr 06:44:26
P1 ΔV	11.384 m/s	11.384 m/s	11.384 m/s
A2 epoch	29-Apr 03:56:45	29-Apr 03:56:57	29-Apr 03:56:26
P2 epoch	3-May 01:07:57	3-May 01:08:23	3-May 01:07:21
A3 epoch	7-May 11:17:45	7-May 11:18:39	7-May 11:17:04
P3 epoch	11-May 18:48:57	11-May 18:50:34	11-May 18:48:11
A4 epoch	16-May 02:57:37	16-May 02:59:58	16-May 02:56:45
P4 epoch	20-May 11:11:29	20-May 11:14:36	20-May 11:10:29
A5 epoch	24-May 19:08:53	24-May 19:12:40	24-May 19:07:48
P5 epoch	29-May 03:23:21	29-May 03:27:53	29-May 03:22:10
P5 ΔV	13.795 m/s	14.762 m/s	13.813 m/s
Moon TCA	1-Jun 21:59:32	1-Jun 21:59:40	1-Jun 21:59:32

Table 6: Five-Loop Trajectory Comparison, +3-Sigma Case. Times are UTC.

	Astrogator	DPTRAJ JGM-3
A1 epoch	22-Apr 11:07:21	22-Apr 11:07:00
A1 ΔV	5.4143 m/s	5.4209 m/s
P1 epoch	26-Apr 09:35:34	26-Apr 09:35:34
P1 ΔV	0.18219 m/s	0.18219 m/s
A2 epoch	30-Apr 06:53:17	30-Apr 06:52:57
P2 epoch	4-May 04:08:04	4-May 04:07:24
A3 epoch	8-May 06:50:07	8-May 06:49:12
P3 epoch	12-May 09:27:54	12-May 09:26:47
A4 epoch	16-May 12:52:57	16-May 12:51:37
P4 epoch	20-May 16:23:10	16-May 16:21:36
A5 epoch	24-May 19:36:11	24-May 19:34:25
P5 epoch	28-May 23:00:52	28-May 22:58:54
P5 ΔV	13.410 m/s	13.483 m/s
Moon TCA	2-Jun 00:14:03	2-Jun 00:14:02

THREE-LOOP TRAJECTORY

Linearization vs. Astrogator Results

Because of the linearization, in order to accept results from LAMBIC it is important to compare them to results from Astrogator. This may be done through LAMBIC's deterministic, or single-sample, mode. By specifying the +3-sigma and –3-sigma injection magnitude errors, this single-sample mode gives results that may be compared to the Astrogator results. Such a comparison is made in Table 7. One should note that there are two principle reasons for the differences: LAMBIC uses a linear approximation to compute the maneuvers and is computing these maneuvers such that the sum of the ΔV magnitudes is a minimum (in addition to the constraint of achieving specified **B•T** and **B•R** values at the Moon).

Table 7: Deterministic LAMBIC results vs. Astrogator output

MVR	+3 sigma		-3 sigma	
	Astrogator	LAMBIC	Astrogator	LAMBIC
P1	4.74 m/s	3.58 m/s	32.7 m/s	34.3 m/s
Pf	19.4 m/s	15.5 m/s	8.14 m/s	10.5 m/s

A table of P1 and Pf maneuver ΔV's as a function of injection ΔV magnitude error, produced using Astrogator, was also available. With the K-file in-hand, it is straightforward to produce linear approximations for the same maneuver strategy. Figure 3, below, shows this linear approximation overlaid on the Astrogator results. This figure is a comparison of linear and nonlinear solutions for the same maneuver strategy.

Figure 3 demonstrates very good agreement for the P1 maneuver, but only moderate agreement for the P3 (Pf) maneuver. Since the variation in the P3 ΔV appears to be linear, one may question this result. The inset blow-up for P3 ΔV shows that the linearized model may fit well very close to the origin but only fits moderately well beyond. Unfortunately, a finer spacing of Astrogator results was not available.

Simulation Results

For all simulations reported on below, LAMBIC performed a 5000 sample Monte Carlo analysis. In addition to mean values, LAMBIC can produce ΔV tabulations at any given percentile level; for the Nth percentile level, there is an N% chance that the actual ΔV magnitude will be smaller. In order to clearly show how the individual models affect the estimate of required ΔV, a progression of solutions is presented, beginning with maneuvers that compensate for only the injection error.

Two different specifications were given for the injection dispersion. The first was 11.6 m/s (3-σ) magnitude error and 2° (3-σ) pointing error. The second was a full-state covariance for the five-loop April-18th trajectory. Results for the former are given in Table 8 and for the latter in Table 9. Accounting for OD error does not influence the results much, even at the 99th percentile. On the other hand, the maneuver execution error has great influence on the results, primarily because execution errors can't be corrected until the Pf maneuver. The Pf maneuver is at the final perigee and, as such, has much less maneuver capability than, say, a maneuver at P2. No simulations with a P2 maneuver have been made, but one should expect use of a maneuver at P2 to lower the total ΔV cost.
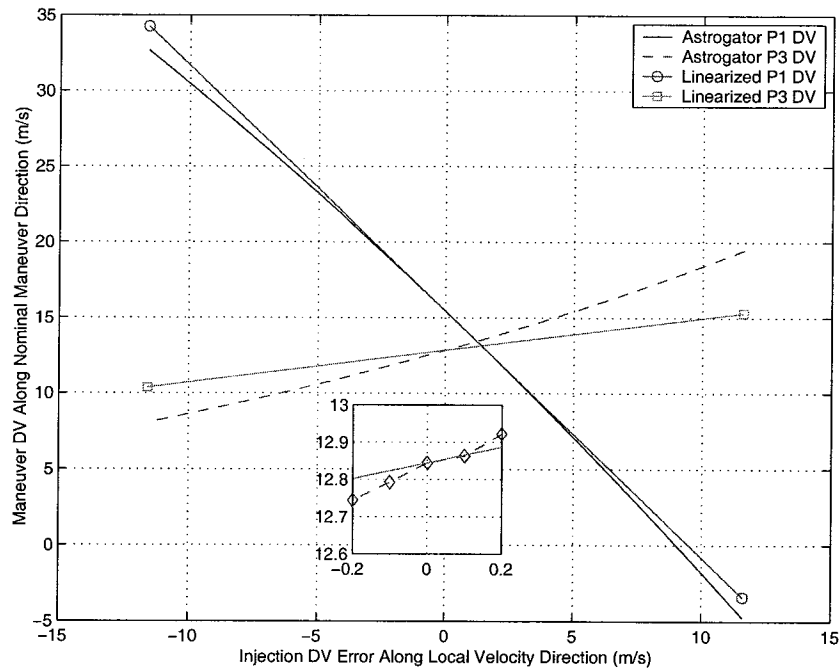

Figure 3. Linearization and Astrogator Comparison. Inset is a blow-up in the region (-0.2 m/s to 0.2 m/s) in injection ΔV by (12.6 m/s to 13 m/s) in P3 ΔV

9

Table 8: LAMBIC Results for Injection Error Dispersion (11.6 m/s, 2° 3-σ). Results are given in m/s. Mean ΔV is listed as μ, standard deviation (1-σ) as σ, and the 99th percentile level is listed under 99%.

MVR	Injection			Injection + OD Error			Injection + Execution Error			Injection + Execution Error + OD Error		
	μ	σ	99%	μ	σ	99%	μ	σ	99%	μ	σ	99%
P1	16.6	6.95	35.3	16.6	6.95	35.4	16.6	6.96	35.3	16.6	6.96	35.3
Pf	13.1	1.82	17.3	13.3	1.83	17.9	17.9	7.60	48.6	18.0	7.61	49.8
Pf CM	0.0	0.0	0.0	0.51	0.29	1.36	1.99	2.07	10.5	2.13	2.04	10.4
Total	29.6	6.43	47.6	30.4	6.47	49.0	36.5	13.2	84.1	36.7	13.1	83.8

It is also important to take note of the delivery dispersion at the lunar swingby, because this analysis assumes that a maneuver strategy that arrives at the correct lunar B-plane aimpoint is representative of one that will also deliver the spacecraft to an appropriate orbit around L2. This assumption must be made because the MAP team will choose a new swingby aimpoint during flight operations based on engineering judgement; this cannot be modeled in LAMBIC. The assumption will be valid, for example, if the chosen aimpoint is close to the nominal or if a delivery to the nominal aimpoint could be followed by a post-lunar-swingby maneuver to achieve the desired L2 orbit. Note that no attempt has been made here to estimate the ΔV required of such a maneuver.

Table 9: LAMBIC Results for Injection Covariance. Results are given in m/s. Mean ΔV is listed as μ, standard deviation (1-σ) as σ, and the 99th percentile level is listed under 99%.

MVR	Injection			Injection + OD Error			Injection + Execution Error			Injection + Execution Error + OD Error		
	μ	σ	99%	μ	σ	99%	μ	σ	99%	μ	σ	99%
P1	15.6	5.38	28.2	15.6	5.38	28.3	15.6	5.39	28.3	15.6	5.39	28.3
Pf	13.0	1.11	15.4	13.2	1.14	15.6	16.9	5.27	36.7	17.1	5.39	37.8
Pf CM	0.0	0.0	0.0	0.51	0.29	1.37	1.87	1.80	8.82	2.03	1.81	9.00
Total	28.5	4.93	40.2	29.3	4.97	41.2	34.4	9.48	65.3	34.7	9.56	67.2

The lunar delivery dispersions reported by LAMBIC are listed in Table 10, for the full injection covariances. The full delivery covariance is listed in the appendix but these standard deviations give a sense of the delivery. The S•R and S•T entries represent angular displacements of the hyperbolic approach hyperbola in the R and T directions. The C3 variation may be converted to V_∞ with the following formula: $\delta V_\infty = \delta C3/(2*$ $V_\infty)$. The nominal V_∞ is about 0.863 km/s, so a standard deviation of 0.001 km²/s² for C3 means V_∞ has a standard deviation of about 0.58 m/s. The LTF entries represent linearized time-of-flight, which is the (hypothetical) rectilinear time-to-go from the current spacecraft position to the center of the target body; the standard deviation of LTF

is usually quite close to the standard deviation of time-of-closest approach. The equation for computing LTF is given, below:

$$t - T_L = \frac{\mu}{v_\infty^3}\left(F_L - \sinh(F_L)\right) \quad where \quad \cosh(F_L) = 1 + \frac{rv_\infty^2}{\mu}$$

where T_L is LTF, t is the current time, μ is the gravitational parameter, r is radius, v_∞ is v-infinity, and F_L is a parameter defined as stated.

Table 10: LAMBIC Lunar B-Plane Delivery Standard Deviations (1-σ) for Injection Covariance.

MVR	Injection	Injection + OD Error	Injection + Execution Error	Injection + Execution Error + OD Error
B•R	0.00	0.922 km	20.3 km	21.4 km
B•T	0.00	2.57 km	37.8 km	40.2 km
LTF	487 s	505 s	487 s	505 s
S•R	3.95 mrad	3.98 mrad	4.35 mrad	4.38 mrad
S•T	15.0 mrad	15.3 mrad	21.2 mrad	21.4 mrad
C3	9.00e-3 km²/s²	9.04e-3 km²/s²	9.97e-3 km²/s²	1.00e-2 km²/s²

20 mrad ≈ 1.15 degrees

FIVE-LOOP TRAJECTORY

Linearization vs. Astrogator Results

The results from LAMBIC are listed in Table 11. Unfortunately, no suitable results from Astrogator were available for comparison. Note that the three Astrogator trajectories for which results are listed in Table 2 do not achieve identical lunar swingby aimpoints and, as such, cannot be used here. The similarities between the ΔV magnitudes listed in Table 11 and those in Table 2 are, however, encouraging.

Table 11: Linearized Modeling of LAMBIC

MVR	-3 sigma	Nominal	+3 sigma
A1	8.18 m/s	6.96 m/s	5.73 m/s
P1	23.6 m/s	11.4 m/s	.787 m/s
Pf	16.6 m/s	13.8 m/s	11.0 m/s

No claim is being made here as to the linear range of this problem. There are, however, reasons to be suspicious. For example, referring to the cases represented in Table 2, the +3-sigma case has a much greater perturbation due to the Moon just before A3 than the nominal case does.

11

Simulation Results

Again, for all simulations reported on below, LAMBIC performed a 5000 sample Monte Carlo analysis. And, the same two injection dispersions were used as for the three-loop. Results for the (11.6 m/s, 2° 3-σ) dispersion are given in Tables 12-14 and for the full 6×6 covariance in Tables 15-17. These results also include simulations of a maneuver at A2 and another at P2.

Accounting for OD error influences the results more than it did for the three-loop trajectory, especially at the 99th percentile. On the other hand, the maneuver execution error has even greater influence on the results, primarily when execution errors aren't corrected until the Pf maneuver. This influence is much larger than in the three-loop case simply because there are two more loops between P1 and Pf. The Pf maneuver is at the final perigee and, as such, has much less maneuver capability than, say, a maneuver at A2 or P2. This difference is illustrated by the simulations that include A2 and P2, seen in Tables 13, 14, 16, and 17. In fact, adding a maneuver at A2 brings the 99th percentile ΔV near the value seen for the three-loop.

The lunar delivery dispersions reported by LAMBIC are listed in Tables 18-20. Full delivery covariances are listed in the appendix, but these standard deviations give a sense of the delivery. The **S•R** and **S•T** entries represent angular displacements of the hyperbolic approach hyperbola in the **R** and **T** directions. The C3 variation may be converted to V_∞ with the following formula: $\delta V_\infty = \delta C3/(2* V_\infty)$. The nominal V_∞ is about 0.814 km/s, so a standard deviation of 0.01 km^2/s^2 for C3 means V_∞ has a standard deviation of about 6.1 m/s.

Table 12: LAMBIC Results for Injection Error Dispersion (11.6 m/s, 2° 3-σ).
Results are given in m/s. Mean ΔV is listed as μ, standard deviation (1-σ) as σ, and the 99th percentile level is listed under 99%.

MVR	Injection			Injection + OD Error			Injection + Execution Error			Injection + Execution Error + OD Error		
	μ	σ	99%	μ	σ	99%	μ	σ	99%	μ	σ	99%
A1	6.95	.431	7.95	6.95	.431	7.95	6.95	.444	8.00	6.95	.444	8.00
P1	11.4	4.02	20.6	11.4	4.02	20.6	11.4	4.03	20.7	11.4	4.03	20.8
Pf	13.8	.938	15.9	23.4	10.3	57.1	45.3	34.0	164	49.2	35.9	172
Pf CM	0.0	0.0	0.0	.094	.070	.308	4.77	6.13	28.4	5.25	6.54	30.8
Total	32.1	5.36	44.4	41.8	11.4	77.1	68.4	40.2	204	72.8	42.0	219

Table 13: LAMBIC Results for Injection Error Dispersion (11.6 m/s, 2° 3-σ) with A2 maneuver. Results are given in m/s. Mean ΔV is listed as μ, standard deviation (1-σ) as σ, and the 99th percentile level is listed under 99%.

MVR	Injection			Injection + OD Error			Injection + Execution Error			Injection + Execution Error + OD Error		
	μ	σ	99%	μ	σ	99%	μ	σ	99%	μ	σ	99%
A1	6.95	.431	7.95	6.95	.431	7.95	6.95	.444	8.00	6.95	.444	8.00
P1	11.4	4.02	20.6	11.4	4.31	20.6	11.4	4.03	20.7	11.4	4.03	20.8
A2	0	0	0	2.09	1.77	7.32	5.39	4.92	22.0	5.96	5.16	22.4
Pf	13.8	.938	15.9	13.9	.963	16.2	14.0	1.08	16.8	14.0	1.10	16.8
Pf CM	0	0	0	.096	.070	.309	.949	.674	3.03	.958	.676	3.02
Total	32.1	5.36	44.4	34.4	5.63	48.2	38.6	8.79	63.6	39.2	8.80	64.3

Table 14: LAMBIC Results for Injection Error Dispersion (11.6 m/s, 2° 3-σ) with P2 maneuver. Results are given in m/s. Mean ΔV is listed as μ, standard deviation (1-σ) as σ, and the 99th percentile level is listed under 99%.

MVR	Injection			Injection + OD Error			Injection + Execution Error			Injection + Execution Error + OD Error		
	μ	σ	99%	μ	σ	99%	μ	σ	99%	μ	σ	99%
A1	6.95	.431	7.95	6.95	.431	7.95	6.95	.444	8.00	6.95	.444	8.00
P1	11.4	4.02	20.6	11.4	4.02	20.6	11.4	4.03	20.7	11.4	4.03	20.8
P2	0	0	0	.082	.061	.259	.140	.123	.552	.166	.135	.601
Pf	13.8	.938	15.9	23.2	9.92	56.4	13.8	1.04	16.5	23.3	9.98	56.9
Pf CM	0	0	0	.096	.070	.309	.941	.658	2.99	2.22	2.26	11.2
Total	32.1	5.36	44.4	41.7	11.1	75.3	33.2	5.61	46.2	44.0	12.5	82.2

Table 15: LAMBIC Results for Injection Covariance. Results are given in m/s. Mean ΔV is listed as μ, standard deviation (1-σ) as σ, and the 99th percentile level is listed under 99%.

MVR	Injection			Injection + OD Error			Injection + Execution Error			Injection + Execution Error + OD Error		
	μ	σ	99%	μ	σ	99%	μ	σ	99%	μ	σ	99%
A1	6.95	.316	7.69	6.95	.316	7.69	6.96	.338	7.73	6.96	.338	7.73
P1	11.3	3.05	18.4	11.3	3.05	18.4	11.3	3.06	18.4	11.3	3.06	18.4
Pf	13.8	.709	15.4	23.4	10.1	56.2	44.6	31.2	151	48.3	33.4	159
Pf CM	0.0	0.0	0.0	.971	.071	.306	4.74	5.87	27.9	5.14	6.29	31.4
Total	32.1	4.06	41.5	41.8	10.8	75.6	67.7	36.6	189	71.8	38.8	203

Table 16: LAMBIC Results for Injection Covariance with A2 maneuver. Results are given in m/s. Mean ΔV is listed as μ, standard deviation (1-σ) as σ, and the 99th percentile level is listed under 99%.

MVR	Injection			Injection + OD Error			Injection + Execution Error			Injection + Execution Error + OD Error		
	μ	σ	99%	μ	σ	99%	μ	σ	99%	μ	σ	99%
A1	6.95	.316	7.69	6.95	.316	7.69	6.96	.338	7.73	6.96	.338	7.73
P1	11.3	3.05	18.4	11.3	3.05	18.4	11.3	3.06	18.4	11.3	3.06	18.4
A2	0	0	0	2.10	1.73	7.15	5.30	4.57	20.5	5.85	4.86	21.2
Pf	13.8	.709	15.4	13.9	.737	15.6	14.0	.876	16.2	14.0	.893	16.3
Pf CM	0	0	0	.097	.071	.306	.956	.663	2.95	.963	.669	2.97
Total	32.1	4.06	41.5	34.4	4.43	44.8	38.5	7.22	59.3	39.1	7.34	60.0

Table 17: LAMBIC Results for Injection Covariance with P2 maneuver. Results are given in m/s. Mean ΔV is listed as μ, standard deviation (1-σ) as σ, and the 99th percentile level is listed under 99%.

MVR	Injection			Injection + OD Error			Injection + Execution Error			Injection + Execution Error + OD Error		
	μ	σ	99%	μ	σ	99%	μ	σ	99%	μ	σ	99%
A1	6.95	.316	7.69	6.95	.316	7.69	6.96	.338	7.73	6.96	.338	7.73
P1	11.3	3.05	18.4	11.3	3.05	18.4	11.3	3.06	18.4	11.3	3.06	18.4
P2	0	0	0	.081	.061	.259	.138	.114	.508	.164	.128	.560
Pf	13.8	.710	15.4	23.3	10.2	56.3	13.8	.817	15.8	23.6	10.3	57.8
Pf CM	0	0	0	.097	.071	.306	.938	.643	2.92	2.29	2.28	11.0
Total	32.1	4.06	41.5	41.8	10.8	75.4	33.2	4.27	43.1	44.3	12.4	84.1

CONCLUDING REMARKS

This analysis culminates in estimating the 99th percentile of ΔV required for the phasing loop legs of two trajectories for the MAP mission. These estimates are subject to several caveats, most notably the reliance on linear approximation. Furthermore, the Pf and PfCM maneuver targets were taken to be the nominal lunar-swingby aimpoint. The resulting estimates of required ΔV are subject to the assumption that achieving this aimpoint is a good approximation to the MAP maneuver strategy.

The trajectory after the Moon has been ignored. No attempt has been made to estimate the ΔV required for any maneuvers after the lunar swingby. There has been no determination as to whether or not a given sample from the Monte Carlo simulation achieves a lissajous orbit. Furthermore, this analysis makes no attempt to estimate the ΔV required to achieve a lissajous orbit after the lunar swingby.

For the five-loop, the results show that a maneuver at A2 or P2 is desirable for keeping the 99th percentile ΔV low. The three-loop case did not show such sensitivity because it had no more than one perigee passage without a maneuver. Clearly, the five-loop case cannot achieve the performance of the three-loop case without an additional maneuver. Furthermore, this maneuver is considerably less expensive if placed at an apogee, viz. A2, as opposed to a perigee, viz. P2.

Table 18: LAMBIC Lunar B-Plane Delivery Standard Deviations (1-σ) for Injection Covariance.

MVR	Injection	Injection + OD Error	Injection + Execution Error	Injection + Execution Error + OD Error
B•R	0.00 km	.775 km	45.2 km	49.3 km
B•T	0.00 km	1.39 km	65.0 km	69.1 km
LTF	4,540 s	4,570 s	4,940 s	4,980 s
S•R	1.81 mrad	1.88 mrad	2.35 mrad	2.44 mrad
S•T	39.8 mrad	42.6 mrad	55.6 mrad	58.2 mrad
C3	$1.32e\text{-}2\ km^2/s^2$	$1.43e\text{-}2\ km^2/s^2$	$1.99e\text{-}2\ km^2/s^2$	$2.10e\text{-}2\ km^2/s^2$

Table 19: LAMBIC Lunar B-Plane Delivery Standard Deviations (1-σ) for Injection Covariance with A2 maneuver.

MVR	Injection	Injection + OD Error	Injection + Execution Error	Injection + Execution Error + OD Error
B•R	0.00 km	.77 km	6.84 km	6.94 km
B•T	0.00 km	1.39 km	10.2 km	10.4 km
LTF	4,540 s	4,550 s	4,580 s	4,590 s
S•R	1.81 mrad	2.45 mrad	4.68 mrad	5.03 mrad
S•T	39.8 mrad	39.8 mrad	39.9 mrad	40.0 mrad
C3	$1.32e\text{-}2\ km^2/s^2$	$1.38e\text{-}2\ km^2/s^2$	$1.68e\text{-}2\ km^2/s^2$	$1.74e\text{-}2\ km^2/s^2$

Table 20: LAMBIC Lunar B-Plane Delivery Standard Deviations (1-σ) for Injection Covariance with P2 maneuver.

MVR	Injection	Injection + OD Error	Injection + Execution Error	Injection + Execution Error + OD Error
B•R	0.00 km	.775 km	6.64 km	18.0 km
B•T	0.00 km	1.39 km	9.98 km	27.3 km
LTF	4,540 s	4,560 s	4,570 s	4,630 s
S•R	1.81 mrad	1.88 mrad	1.82 mrad	1.91 mrad
S•T	39.8 mrad	42.2 mrad	40.0 mrad	42.6 mrad
C3	$1.32e\text{-}2\ km^2/s^2$	$1.41e\text{-}2\ km^2/s^2$	$1.33e\text{-}2\ km^2/s^2$	$1.44e\text{-}2\ km^2/s^2$

APPENDIX

DPTRAJ K-File Modification

The DPTRAJ K-file had to be modified to account for the synchronization of maneuvers with perigees. The modification is straightforward, considering how individual perturbations affect the target B-plane parameters.

$$\delta \mathbf{b} = \frac{d\mathbf{b}}{d\mathbf{v}_{inj}}\delta \mathbf{v}_{inj} + \frac{d\mathbf{b}}{d\mathbf{v}_{a1}}\delta \mathbf{v}_{a1} + \frac{d\mathbf{b}}{d\mathbf{v}_{p1}}\delta \mathbf{v}_{p1} + \frac{d\mathbf{b}}{d\mathbf{v}_{a1}}\delta \mathbf{v}_{a2} + \frac{d\mathbf{b}}{d\mathbf{v}_{p1}}\delta \mathbf{v}_{p2} + \frac{d\mathbf{b}}{d\mathbf{v}_{pf}}\delta \mathbf{v}_{pf} + \cdots$$

$$\frac{d\mathbf{b}}{dt_{a1}}\delta t_{a1} + \frac{d\mathbf{b}}{dt_{p1}}\delta t_{p1} + \frac{d\mathbf{b}}{dt_{pf}}\delta t_{pf}$$

where **b** is a vector of the B-plane target parameters; $\mathbf{v}_{inj}$, $\mathbf{v}_{p1}$, and $\mathbf{v}_{pf}$ are the velocity vectors at the maneuver times; t_{p1} and t_{pf} denote the times of the P1 and Pf maneuvers, respectively. The K-matrices that DPTRAJ writes to the K-file are the partial derivatives between velocity and B-plane targets.

The requirements that the P1 and Pf maneuvers be placed at perigees are expressed as follows:

$$\delta t_{a1} = \frac{dt_{a1}}{d\mathbf{v}_{inj}}\delta \mathbf{v}_{inj}$$

$$\delta t_{p1} = \frac{dt_{p1}}{d\mathbf{v}_{inj}}\delta \mathbf{v}_{inj} + \frac{dt_{p1}}{d\mathbf{v}_{a1}}\delta \mathbf{v}_{a1} + \frac{dt_{p1}}{dt_{a1}}\delta t_{a1}$$

$$\delta t_{pf} = \frac{dt_{pf}}{d\mathbf{v}_{inj}}\delta \mathbf{v}_{inj} + \frac{dt_{pf}}{d\mathbf{v}_{a1}}\delta \mathbf{v}_{a1} + \frac{dt_{pf}}{dt_{a1}}\delta t_{a1} + \frac{dt_{pf}}{d\mathbf{v}_{a2}}\delta \mathbf{v}_{a2} + \frac{dt_{pf}}{d\mathbf{v}_{p1}}\delta \mathbf{v}_{p1} + \frac{dt_{pf}}{dt_{p1}}\delta t_{p1} + \frac{dt_{pf}}{d\mathbf{v}_{p2}}\delta \mathbf{v}_{p2}$$

Note that these equations express the variation in perigee times due to variations in maneuver time and ΔV. Substituting these, as constraints on the times of maneuvers, back into the first equation, yields:

16

$$\delta b = \left[\begin{array}{l} \dfrac{d\mathbf{b}}{d\mathbf{v}_{inj}} + \dfrac{d\mathbf{b}}{dt_{a1}}\dfrac{dt_{a1}}{d\mathbf{v}_{inj}} + \dfrac{d\mathbf{b}}{dt_{p1}}\dfrac{dt_{p1}}{d\mathbf{v}_{inj}} + \dfrac{d\mathbf{b}}{dt_{pf}}\dfrac{dt_{pf}}{d\mathbf{v}_{inj}} + \dfrac{d\mathbf{b}}{dt_{p1}}\dfrac{dt_{p1}}{dt_{a1}}\dfrac{dt_{a1}}{d\mathbf{v}_{inj}} \\[2ex] + \dfrac{d\mathbf{b}}{dt_{pf}}\dfrac{dt_{pf}}{dt_{a1}}\dfrac{dt_{a1}}{d\mathbf{v}_{inj}} + \dfrac{d\mathbf{b}}{dt_{pf}}\dfrac{dt_{pf}}{dt_{p1}}\dfrac{dt_{p1}}{d\mathbf{v}_{inj}} + \dfrac{d\mathbf{b}}{dt_{pf}}\dfrac{dt_{pf}}{dt_{p1}}\dfrac{dt_{p1}}{dt_{a1}}\dfrac{dt_{a1}}{d\mathbf{v}_{inj}} \end{array}\right]\delta\mathbf{v}_{inj} + \cdots$$

$$\left[\dfrac{d\mathbf{b}}{d\mathbf{v}_{a1}} + \dfrac{d\mathbf{b}}{dt_{p1}}\dfrac{dt_{p1}}{d\mathbf{v}_{a1}} + \dfrac{d\mathbf{b}}{dt_{pf}}\dfrac{dt_{pf}}{d\mathbf{v}_{a1}} + \dfrac{d\mathbf{b}}{dt_{pf}}\dfrac{dt_{pf}}{dt_{p1}}\dfrac{dt_{p1}}{d\mathbf{v}_{a1}}\right]\delta\mathbf{v}_{a1} + \cdots$$

$$\left[\dfrac{d\mathbf{b}}{d\mathbf{v}_{p1}} + \dfrac{d\mathbf{b}}{dt_{pf}}\dfrac{dt_{pf}}{d\mathbf{v}_{p1}}\right]\delta\mathbf{v}_{p1} + \left[\dfrac{d\mathbf{b}}{d\mathbf{v}_{a2}} + \dfrac{d\mathbf{b}}{dt_{pf}}\dfrac{dt_{pf}}{d\mathbf{v}_{a2}}\right]\delta\mathbf{v}_{a2} + \cdots$$

$$\left[\dfrac{d\mathbf{b}}{d\mathbf{v}_{p2}} + \dfrac{d\mathbf{b}}{dt_{pf}}\dfrac{dt_{pf}}{d\mathbf{v}_{p2}}\right]\delta\mathbf{v}_{p2} + \dfrac{d\mathbf{b}}{d\mathbf{v}_{pf}}\delta\mathbf{v}_{pf}$$

These six coefficient matrices for the velocity increments may then be used as replacement K-matrices. The altitude constraint is handled without loss of generality by considering it as one of the target parameters in the vector **b**.

LAMBIC Delivery Covariances

The delivery standard deviations reported in the "Injection + Execution Error + OD Error" columns of Tables 10, 18, and 19 are taken from the covariance matrices quoted below in lower diagonal form. The row-order , reading top to bottom, is **B•R**(km), **B•T** (km), LTF (days), **S•R** (radians), **S•T** (radians), and C3 (km²/s²).

Three-Loop for Injection Covariance (injection+maneuver+OD errors.

```
 4.60010E+02
 2.59487E+02   1.61951E+03
 2.64392E+02  -1.42087E+02   2.55005E+05
-1.02918E-03   1.25991E-03  -1.34326E+00   1.91634E-05
 7.37874E-04   1.91690E-02   6.96660E-01   6.64345E-05   4.58277E-04
-3.95513E-03   1.99451E-03  -2.50407E+00   4.30570E-05   1.68732E-04   9.99801E-05
```

Five-Loop for Injection Covariance.

```
 2.4272e+03
 8.7658e+02   4.7738e+03
 4.9198e+03   6.3116e+02   2.4824e+07
 6.8699e-03   5.4289e-03   3.6631e+00   5.9508e-06
-5.4620e-02   9.8834e-02   1.2962e+02   7.4628e-05   3.3866e-03
 1.9949e-03  -5.7947e-02  -4.9959e+01  -3.1534e-05  -1.1865e-03   4.4253e-04
```

17

Five-Loop for Injection Covariance with A2 maneuver.
```
 4.8214e+01
 2.0827e+01   1.0859e+02
-5.5448e+02   3.0504e+01   2.1040e+07
-2.4965e-04  -9.1431e-04   6.1763e+00   2.5324e-05
-4.3858e-03   2.7374e-03   1.7394e+02  -3.9297e-06   1.5999e-03
 5.6144e-04  -3.2077e-03  -5.2300e+01   4.7168e-05  -5.7159e-04   3.0192e-04
```

Injection Covariance

```
MAP MISSION 18 APRIL 2001
  COVARIANCE MATRIX OF TECO      INJECTION CONDITIONS BASED ON -3 SIGMA SENSITIVITIES
                                 X                  Y                  Z
                                 FEET               FEET               FEET

     X          FEET          0.11916690E+10     -0.56301814E+06    -0.28119734E+06
     Y          FEET         -0.56301814E+06      0.12767127E+08     0.46452044E+06
     Z          FEET         -0.28119734E+06      0.46452044E+06     0.80101014E+07
     VX         FT/SEC        0.11494819E+05     -0.63863203E+03    -0.58089530E+04
     VY         FT/SEC       -0.42820439E+03      0.59201057E+04     0.24453652E+03
     VZ         FT/SEC       -0.14129451E+07      0.79088917E+03     0.89430986E+04
     THETA LP   DEGREES       0.31790254E+04     -0.15083154E+01    -0.75353125E+00
     PSI   LP   DEGREES       0.23994196E+03      0.16904696E+01     0.23692084E-01
                                 VX                 VY                 VZ
                                 FT/SEC             FT/SEC             FT/SEC

     X          FEET          0.11494819E+05     -0.42820439E+03    -0.14129451E+07
     Y          FEET         -0.63863203E+03      0.59201057E+04     0.79088917E+03
     Z          FEET         -0.58089530E+04      0.24453652E+03     0.89430986E+04
     VX         FT/SEC        0.95635289E+02     -0.27066217E+02    -0.29768523E+02
     VY         FT/SEC       -0.27066217E+02      0.33453510E+04     0.15188399E+00
     VZ         FT/SEC       -0.29768523E+02      0.15188399E+00     0.50315726E+04
     THETA LP   DEGREES      -0.51418243E-01     -0.33268598E-02     0.15235504E+02
     PSI   LP   DEGREES       0.15368232E+00     -0.19005207E+02    -0.28228162E+00
```

Positive x axis is parallel to the projection of the vehicle's instantaneous velocity vector onto a plane perpendicular to the radius vector. Z is positive away from the earth along the radius vector. Y completes the right-handed orthogonal system. The origin is at the nominal vehicle present position point and the system is inertial.

B-Plane Description

Planet or satellite approach trajectories are typically described in aiming plane coordinates referred to as "*B*–plane" coordinates (see Figure 4).[7] The B-plane is a plane passing through the planet center and perpendicular to the asymptote of the incoming trajectory (assuming 2 body conic motion). The "B-vector" is a vector in that plane, from the planet center to the piercing-point of the trajectory asymptote. The B-vector specifies where the point of closest approach would be if the target planet had no mass and did not deflect the flight path. Coordinates are defined by three orthogonal unit vectors, *S*, *T*, and *R*, with the system origin at the center of the target body. The *S* vector is parallel to the incoming spacecraft V_∞ vector (approximately the velocity vector at the time of entry into the gravitational sphere of influence). *T* is arbitrary, but is typically specified to lie in the ecliptic plane (the mean plane of the Earth's orbit), or in a body-equatorial plane. Finally, *R* completes an orthogonal triad with *S* and *T*.
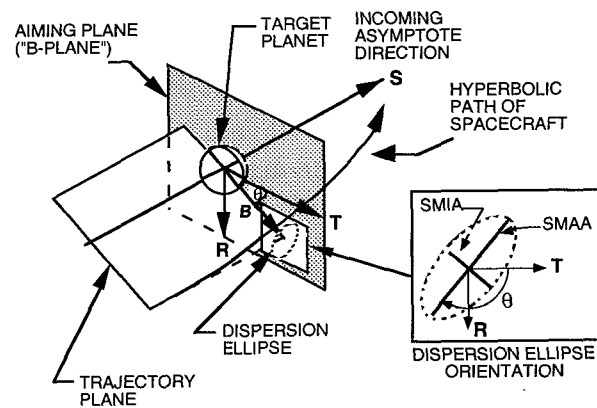
Figure 4: B-Plane Coordinate System

Trajectory errors in the B-plane are often characterized by a one–σ dispersion ellipse, shown in Figure 4. SMAA and SMIA denote the semi–major and semi–minor axes of the ellipse; θ is the angle measured clockwise from the **T** axis to SMAA. The dispersion normal to the B-plane is typically given as a one-σ *time-of-flight* error, where time-of-flight specifies what the time to swingby (periapsis) would be from some given epoch if the magnitude of the B-vector were zero. Alternatively, this dispersion is sometimes given as a one-σ distance error along the S direction, numerically equal to the time-of-flight error multiplied by the magnitude of the V_∞ vector.

ACKNOWLEDGMENTS

[1] Richon, K. V., Mathews, M. W., "An overview of the Microwave Anisotropy Probe (MAP) Trajectory Design" 1997 AAS/AIAA Astrodynamics Specialist Conference, Sun Valley, Idaho, August 4-7, 1997, paper no. AAS 97-728.

[2] "DPTRAJ-ODP User's Reference Manual, Vol. 1" JPL Internal Document: 630-336, Pasadena, CA.

[3] Maize, E. H., "Linear Statistical Analysis of Maneuver Optimization Strategies," (AAS 87-486) presented at AAS/AIAA Astrodynamics Conference, Kalispell, Montana, August 10-13, 1987.

[4] Gates, C.R., "A Simplified Model of Midcourse Maneuver Execution Errors," JPL Technical Report 32-504, JPL, Pasadena, CA, October 15, 1963.

[5] Nerem, R. S., Lerch, F. J., Marshall, J. A., Pavlis, E. C., Putney, B. H., Tapley, B. D., Eanes, R. J., Ries, J. C., Schutz, B. E., Shum, C. K., Watkins, M. M., Klosko, S. M., Chan, J. C., Luthcke, S. B., Patel, G. B., Pavlis, N. K., Williamson, R. G., Rapp, R. H., Biancale, R., and Nouël, F., "Gravity Model Development for

TOPEX/POSEIDON: Joint Gravity Models 1 and 2", Journal of Geophysical Research, Vol. 99, No. C12, 1994, pp 24,421-24,447.

[6] Tapley, B. D., Watkins, M. M., Ries, J. C., Davis, G. W., Eanes, R. I., Poole, S. R., Rim, J. H., Schutz, B. E., Shum, C. K., Nerem, R. S., Lerch, F.J., Marshall, J. A., Klosko, S. M., Pavlis, N. K., and Wiliamson, R. G., "The JGM-3 Geopotential Model", Journal of Geophysical Research, Vol. 101, No. B12, 1996, pp 28,029-28,049.

[7] Kizner, W., "A Method of Describing Miss Distances for Lunar and Interplanetary Trajectories," JPL External Publication 674, August 1, 1959.